J. Fluid Mech. (1987), *vol.* 178, *pp* 521–534
Printed in Great Britain

Dynamically consistent magnetic fields produced by differential rotation

By D. R. FEARN
Department of Mathematics, University Gardens, Glasgow, G12 8QW, UK

AND M. R. E. PROCTOR
Department of Applied Mathematics and Theoretical Physics, University of Cambridge, Silver Street, Cambridge CB3 9EW, UK

(Received 17 June 1986)

We investigate the dynamical consequences of an axisymmetric velocity field with a poloidal magnetic field driven by a prescribed e.m.f. E. The problem is motivated by previous investigations of dynamically driven dynamos in the magnetostrophic range. A geostrophic zonal flow field is added to a previously described velocity, and determined by the requirement that Taylor's constraint (Taylor 1963) (guaranteeing dynamical self-consistency of the fields) be satisfied. Several solutions are exhibited, and it is suggested that self-consistent solutions can always be found to this 'forced' problem, whereas the usual α-effect dynamo formalism in which E is a linear function of the magnetic field leads to a difficult transcendentally nonlinear characteristic value problem that may not always possess solutions.

1. Introduction

It has long been known that the magnetic field of the Earth (and of some other planets) is maintained by a dynamo mechanism. The effects of advection by motions of the conducting fluid in the core tend to stretch the magnetic field lines and increase the magnetic energy, compensating for resistive effects which turn magnetic energy into heat. The purely kinematic aspects of this problem (in which the velocity field is supposed given, and the magnetic field arises as an instability) have been extensively investigated (for a comprehensive review see Moffatt 1978), but only in recent years has there been significant progress on the much more difficult nonlinear problem in which the velocities are caused by body forces, and are themselves subject to the Lorentz forces exerted by the magnetic field.

Order-of-magnitude estimates of magnetic field strengths in the Earth's core reveal that for the relatively long timescales (of the order of 10^2–10^4 y) associated with the evolution of the main geomagnetic field, the primary force balance is between the Lorentz forces, Coriolis forces and pressure gradients, with inertial forces and viscosity playing a secondary role, except perhaps in the boundary layers. (For example, the Ekman number in the core is probably no larger than 10^{-14}.) Such a regime has become known as 'magnetostrophic'. One can then hope to describe the relevant dynamics with an equation of the form

$$2\rho(\boldsymbol{\Omega} \times \boldsymbol{U}) = -\nabla p + \boldsymbol{F}, \tag{1.1}$$

where $\boldsymbol{F}$ represents the body forces (including the Lorentz force). $\boldsymbol{\Omega}$ the angular velocity of the core, and $\boldsymbol{U}$, p and ρ respectively the relative velocity, pressure and

density. It is clear that if (1.1) has a solution (in a sphere, say, satisfying $\boldsymbol{U}\cdot\boldsymbol{n}=0$ on the surface where $\boldsymbol{n}$ is the outward normal) then $\boldsymbol{U}$ is determined only up to an arbitrary geostrophic flow $U_{\rm G}(s)\,\hat{\boldsymbol{\phi}}$, where s is the distance from the rotation axis. Such a lack of uniqueness suggests, from a mathematical point of view, that (1.1) may not always possess solutions for arbitrary $\boldsymbol{F}$, and indeed Taylor (1963) showed that for a solution to exist the zonal component of $\boldsymbol{F}$ is required to satisfy the conditions

$$\int_{C(s)} F_\phi(s,z)\,\mathrm{d}z\,\mathrm{d}\phi \equiv T(s)=0, \tag{1.2}$$

where $C(s)$ is any cylinder coaxial with the rotation axis inscribed in the sphere.

Taylor showed how to determine $U_{\rm G}$ up to a solid-body rotation as the solution of an initial-value problem when the induction equation was taken into account and an initial field chosen to satisfy (1.1). Interest then focused on whether a self-excited field $\boldsymbol{B}$ could be found, together with a corresponding flow $U_{\rm G}(s)$, with $\boldsymbol{B}$ satisfying the basic compatibility condition (2.6). Most progress has been made for so-called 'mean-field' models in which the effect of a small-scale or turbulent velocity field on a mean magnetic field $\boldsymbol{B}$ is modelled by a mean e.m.f. $E_i=\alpha_{ij}B_j$ (the 'α-effect') in the induction equation for $\boldsymbol{B}$. Problems of this type have been investigated by Childress (1969), Malkus & Proctor (1975) and Proctor (1977). Childress showed that trivial solutions (with $U_{\rm G}\equiv 0$) could be found in the special case $\alpha_{ij}=\alpha\delta_{ij}$, with α a constant (although problems arise at higher orders in amplitude, as shown by Proctor 1975), while the other two papers dealt with more realistic forms of the α-effect, and showed that the problem is in general a non-trivial one, with $U_{\rm G}$ being obtained as part of the eigensolution. It has proved hard to formulate a tractable problem, though Greenspan (1974) and Proctor (1975) made some progress in simplified geometries, and more recently Soward & Jones (1983) and Ierley (1985) have approached the problem by reinstating the viscous terms in (1.1) and finding $U_{\rm G}$ as a singular limit as the Ekman number goes to zero.

There is still room for doubt, however, as to whether solutions of the required form are possible for general forms of the α-effect. Of course, while $\boldsymbol{E}$ is certainly a linear functional of $\boldsymbol{B}$ it is not obvious that the local relation furnished by the α-effect is ever an accurate representation for realistic velocity fields. Fearn & Proctor (1983*a*, *b*) have undertaken extensive studies of magnetostrophic convection in a sphere, and used them to construct models of mean fields that do not arise as an instability according to the ideas of the kinematic theory, but are driven directly by a non-axisymmetric instability, which relies for its energy on unstable entropy gradients. Preliminary calculations are reported in Fearn & Proctor (1984) and a full account is given in Fearn & Proctor (1987); these papers are referred to hereinafter as FP84, FP87. In the latter paper we describe attempts to incorporate the Taylor constraint into our model. Though these have not been wholly successful, they suggested to us that calculations of $U_{\rm G}$ might be made easier were the e.m.f. $\boldsymbol{E}$, rather than the quantity α, prescribed. (In a full solution $\boldsymbol{E}$ would depend on $\boldsymbol{B}$ through the non-axisymmetric convection problem.) Such a prescription in any event appears naturally in the formulation of FP87, where the assumptions leading to the α-effect ansatz cannot be justified. For any given $\boldsymbol{E}$ the calculations yield, besides $U_{\rm G}$ the mean toroidal field B: these can be converted into an α-effect if desired by writing $\alpha=E_\phi/B$. Of course the resulting α may have singularities.

The present paper reports an extensive investigation, making use of the above ideas, into the way in which self-consistent magnetic fields can arise. We concentrate on dynamos of the '$\alpha\omega$' (or, in our case, '$E\omega$') type, in which the poloidal field is

sustained by $\boldsymbol{E}$, while the zonal field is produced from the poloidal field by the action of a differential rotation, which is prescribed, apart from its geostrophic part $U_G\,\hat{\boldsymbol{\phi}}$. The problem is formulated in the next section, and it is shown that it can be reduced to an integral equation of the first kind for $G(s) = s(\mathrm{d}/\mathrm{d}s)\,(U_G/s)$, and further that the form of this equation is such that smooth solutions can be expected. In §3 we give brief details of the method of solution (a fuller description is give in FP87). Results are presented in §4 and we show that solutions for $G(s)$ can indeed be found for a variety of different cases. In a conclusion we discuss the significance of the results.

2. Derivation and structure of the equations

In the self-consistent dynamo model discussed in FP84, FP87, we distinguish sharply, following Braginskii (1975) between axisymmetric and non-axisymmetric fields. The non-axisymmetric magnetic, temperature and velocity fields are supposed to arise as an instability of convective type on an axisymmetric background. The latter is maintained (at least as far as the magnetic field is concerned) by the nonlinear interaction of the non-axisymmetric convection, leading to an axisymmetric e.m.f. of the form $\boldsymbol{E} = \langle \boldsymbol{u} \times \boldsymbol{b} \rangle$, where $\boldsymbol{u}$ and $\boldsymbol{b}$ represent the non-axisymmetric velocity and magnetic fields respectively, and the angle brackets indicate an azimuthal average of each component of the vector in polar coordinates. The theory also requires large differential rotation, which is much more effective in producing a toroidal from a poloidal field than $\boldsymbol{E}$. Then the only important part of $\boldsymbol{E}$ is its azimuthal component (denoted here by E) which is responsible for maintaining the poloidal field. We may then write the axisymmetric part of the dynamo problem addressed in FP87 in the form

$$\left.\begin{aligned} s^{-1}\boldsymbol{U}_{\mathrm{p}}\cdot\nabla(sA) &= E + (\nabla^2 - s^{-2})\,A, \\ s\boldsymbol{U}_{\mathrm{p}}\cdot\nabla\left(\frac{B}{s}\right) &= s\boldsymbol{B}_{\mathrm{p}}\cdot\nabla\left(\frac{U}{s}\right) + (\nabla^2 - s^{-2})\,B, \end{aligned}\right\} \tag{2.1}$$

where we have used cylindrical polar coordinates (s, ϕ, z). [For a derivation see, for example, Moffatt 1978.] The magnetic field

$$\boldsymbol{B}(s,z) = \boldsymbol{B}_{\mathrm{p}} + B\hat{\boldsymbol{\phi}}; \quad \boldsymbol{B}_{\mathrm{p}} = \nabla \times (A\hat{\boldsymbol{\phi}}), \tag{2.2}$$

while the velocity field is similarly decomposed as

$$\boldsymbol{U}(s,z) = \boldsymbol{U}_{\mathrm{p}} + U\hat{\boldsymbol{\phi}}. \tag{2.3}$$

The equations have been non-dimensionalized in such a way that the diffusion coefficient is unity (see FP84, FP87 for details). Equations (2.1) are to be solved in a sphere of (dimensionless) unit radius with $\boldsymbol{B}$ matching to an external potential field. For a given $\boldsymbol{E}$ and $\boldsymbol{U}$, $\boldsymbol{B}$ is then determined uniquely. However, the magnetic field that emerges will not in general satisfy the Taylor condition (1.2), with $\boldsymbol{F}$ replaced by the Lorentz force $((\nabla \times \boldsymbol{B}) \times \boldsymbol{B})$. Since the magnetostrophic equation (1.1) only defines $\boldsymbol{U}$ up to a geostrophic flow we are free to add such a flow to $\boldsymbol{U}$ in (2.1) to attempt to achieve consistency. We therefore write, instead of (2.3),

$$\boldsymbol{U} = \boldsymbol{U}_{\mathrm{p}} + (U_0 + s\Omega_{\mathrm{G}}(s))\,\hat{\boldsymbol{\phi}}, \tag{2.4}$$

where $\boldsymbol{U}_{\rm p}$ and U_0 are prescribed. Then the equations to be solved are

$$0 = -sU_{\rm p}\cdot\nabla\left(\frac{B}{s}\right)+sB_{\rm p}\cdot\nabla\left(\frac{U_0}{s}\right)+s(B_{\rm p}\cdot\hat{s})\frac{{\rm d}\Omega_{\rm G}}{{\rm d}s}+\left(\nabla^2-\frac{1}{s^2}\right)B, \tag{2.5a}$$

$$0 = E-\frac{1}{s}U_{\rm p}\cdot\nabla(sA)+\left(\nabla^2-\frac{1}{s^2}\right)A \tag{2.5b}$$

in the sphere $r \leqslant 1$. The geostrophic flow $\Omega_{\rm G}(s)$ is determined (up to an additive constant) by the constraint (cf. (1.2))

$$T(s) \equiv \int_{C(s)} \tau(s,z)\,{\rm d}z = 0, \tag{2.6}$$

where $\tau(s,z) = [(\nabla\times B\hat{\boldsymbol{\phi}})\times(\nabla\times A\hat{\boldsymbol{\phi}})]_{\phi}$. The flows U_0 and $\boldsymbol{U}_{\rm p}$ are to be regarded as the basic (non-magnetic) parts of the mean velocity field. In keeping with the quasi-kinematic nature of the study, we neglect the corrections to U_0 and $\boldsymbol{U}_{\rm p}$ given by the solutions of (2.5).

According to Braginskii (1964*a*, *b*) the driving e.m.f. E (here prescribed) may be related directly to the local value of B in the limit of large $R_{\rm m}$ by the ansatz

$$E = \alpha B, \tag{2.7}$$

where $\alpha(r,\theta)$ depends only on the asymmetric velocity $\boldsymbol{u}$. If (2.7) is substituted into (2.5) the latter becomes a problem that is homogeneous in the magnetic-field amplitude, and then $\Omega_{\rm G}(s)$ may be thought of as an 'eigenflow' that permits satisfaction of (2.6) (Malkus & Proctor 1975; Proctor 1977; Ierley 1985). In this form, or one closely allied, it has received attention from the above authors and also Soward & Jones (1983). All these papers choose the form of α and then investigate the circumstances in which a solution of (2.5), (2.6) can exist. Of course, the *amplitude* of α must be adjusted in this case to obtain a steady solution, and so the problem becomes one of eigenvalue type. Here we have preferred to work with a fixed E, for two reasons. First, (2.8) is not very accurate if $R_{\rm m}$ is not very large and even at large $R_{\rm m}$ it fails at the equator and at points where the zonal phase velocity of the wavelike disturbance represented by $\boldsymbol{u}$, $\boldsymbol{b}$ is very close to the local differential rotation velocity [see FP84]. Secondly, the interest of this forced problem derives from its role in the self-consistent dynamo calculation described in FP87. Then, because it arises from a convection problem whose dynamics are affected by B, the dependence of E on B is much more complicated than the linear relation (2.7). If in our quasi-kinematic study we accept E as prescribed, there is a powerful computational advantage too; for then A is given by E and $\boldsymbol{U}_{\rm p}$, and does not depend on $\Omega_{\rm G}$. We can then see that for fixed U_0, (2.5*a*) can be written as an integral equation of the first kind for the quantity $G(s) = s\,{\rm d}\Omega_{\rm G}/{\rm d}s$, in the following manner. We may write (2.5*a*) in the form

$$L_0 B \equiv -\left(\nabla^2-\frac{1}{s^2}\right)B+sU_{\rm p}\cdot\nabla\left(\frac{B}{s}\right) = sB_{\rm p}\cdot\nabla\left(\frac{U_0}{s}\right)+G(s)\,B_{{\rm p}s}, \tag{2.8}$$

where $B_{{\rm p}s} = \boldsymbol{B}_{\rm p}\cdot\hat{\boldsymbol{s}}$. Since the equation $L_0 B = 0$ has the unique solution $B = 0$, (2.9) has a unique solution that is given (formally) in terms of the Green's function $K(\boldsymbol{x},\boldsymbol{x}')$ of L_0 by

$$B(\boldsymbol{x}) = \int_{r<1} K(\boldsymbol{x},\boldsymbol{x}')\left\{s'\boldsymbol{B}_{\rm p}(\boldsymbol{x}')\cdot\nabla\left(\frac{U_0(\boldsymbol{x}')}{s'}\right)\right\}{\rm d}^2\boldsymbol{x}'+\int_{r<1} K(\boldsymbol{x},\boldsymbol{x}')\,G(s')\,B_{{\rm p}s}(\boldsymbol{x}')\,{\rm d}^2\boldsymbol{x}', \tag{2.9}$$

where $\mathrm{d}^2\boldsymbol{x}' \equiv s'\mathrm{d}s'\mathrm{d}z'$. The first term on the right-hand side is given independently of $G(s)$, so we can write it as $B_0(\boldsymbol{x})$, say. We now apply (2.6), but in the reduced form [which can be obtained from (2.6) by manipulation]

$$\bar{T}(s) \equiv \int_{C(s)} BB_{\mathrm{p}s}\,\mathrm{d}z = 0 \tag{2.10}$$

(see Childress 1969) to yield the result

$$0 = \int_{C(s)} B_0 B_{\mathrm{p}s}\,\mathrm{d}z + \int_0^1 s'\,\mathrm{d}s' \int_{C(s)} \mathrm{d}z \int_{C(s')} \mathrm{d}z' B_{\mathrm{p}s}(s,z)\, B_{\mathrm{p}s}(s',z')\, K(s,z,s',z')\, G(s'), \tag{2.11}$$

or, equivalently,

$$F(s) = \int_0^1 H(s,s')\, G(s')\,\mathrm{d}s', \tag{2.12}$$

where

$$\left.\begin{aligned} F(s) &= -\int_{C(s)} B_0 B_{\mathrm{p}s}\,\mathrm{d}z, \\ H(s,s') &= s' \int_{C(s)} \mathrm{d}z \int_{C(s')} \mathrm{d}z'\, B_{\mathrm{p}s}(s,z)\, B_{\mathrm{p}s}(s',z')\, K(s,z,s',z'). \end{aligned}\right\} \tag{2.13}$$

We can see from the last expression that the problem has been reduced to an integral equation of the first kind. It is easy to show that (2.12) has no non-trivial solutions if $F(s) = 0$. For if $U_0(\boldsymbol{x}) = 0$, we have from (2.5)

$$0 = B_{\mathrm{p}s}\, G(s) - sU_{\mathrm{p}} \cdot \nabla\left(\frac{B}{s}\right) + \left(\nabla^2 - \frac{1}{s^2}\right) B. \tag{2.14}$$

Multiplying through by B/s^2, integrating over s from 0 to 1, and using (2.10), we have

$$\begin{aligned} 0 = \int \frac{G(s)}{s^2}\, BB_{\mathrm{p}s}\,\mathrm{d}^2\boldsymbol{x} &= \int_0^1 \frac{G(s)}{s} \int_{C(s)} BB_{\mathrm{p}s}\,\mathrm{d}z\,\mathrm{d}s \\ &= \int \left[\frac{B}{s}\, U_{\mathrm{p}} \cdot \nabla\left(\frac{B}{s}\right) + \frac{B}{s^2}\left(\nabla^2 - \frac{1}{s^2}\right) B\right] \mathrm{d}^2\boldsymbol{x}. \end{aligned} \tag{2.15}$$

The first term in the last expression vanishes since $\nabla \cdot \boldsymbol{U}_{\mathrm{p}} = 0$, while the second can be shown to be negative definite by routine manipulations (see e.g. Moffatt 1978). Thus we have a contradiction; this implies that when $U_0(\boldsymbol{x}) \neq 0$ (2.12) has a unique solution, and the only question is whether the solution $G(s)$ is sufficiently well behaved to count as a realistic flow. The answer to this question depends on the smoothness of the function $F(s)$ and of the kernel $H(s,s')$, but though we have been able to find no rigorous proof that G is smooth it seems clear from the form of $F(s)$, which is essentially that of kernel similar to H acting on $U_0(\boldsymbol{x})$, that a smooth solution is possible, and indeed none of our computations shows any evidence of discontinuities in $G(s)$.

It is important to note, however, that the smooth solution that is found is $G(s) = s\,\mathrm{d}\Omega_{\mathrm{G}}/\mathrm{d}s$, and there is no reason why $G(s)$ should vanish at $s = 0$. Thus typically Ω_{G} will have a logarithmic singularity there. Such a solution should not alarm us, however, since there is no viscosity in the problem and so infinite shears are certainly permitted. The singularity is not very severe (U_{G} remains finite) and in the presence of viscosity would be accommodated by a passive boundary layer near the axis of symmetry. A similar singularity was found for the simplified dynamo model in a cylindrical geometry discussed by Proctor (1975) for which $G(s) = \text{const.}$

3. Numerical solution

Instead of solving (2.12), (2.13) directly, we choose to work with (2.5) and (2.6). We write

$$G(s) = \sum_{n=1}^{N_T} G_n T_n(x), \quad x = 2s-1, \tag{3.1}$$

where the $T_n(x)$ are Chebyshev polynomials, so that $-1 \leqslant x \leqslant 1$. This representation is used in two different ways, explained fully in §4.2; either $G(s)$ is represented by the sum (3.1) for $0 \leqslant s \leqslant 1$, or the representation is used only for $0 \leqslant s \leqslant s_0 < 1$, with $G(s)$ having a linear form for $s_0 \leqslant s \leqslant 1$ with G and G' continuous at s_0. In either case, G is given in terms of N_T undetermined coefficients. Adequate resolution was achieved with $N_T = 7$ in most cases, though higher values were used to check convergence. With given values of E and U_p, (2.5*b*) was then solved for A on a spherical polar mesh, with A being matched to the potential of an exterior irrotational field outside the 'core', in the usual way. The method used for this solution is described fully in FP84, but is entirely straightforward. Then (2.5*a*) was solved, with a given U_0, for B, with the boundary condition $B = 0$ at $r = 1$. B therefore depends on the coefficients G_n in a complicated way. We next evaluate

$$T_S = \left[\frac{1}{N_s}\sum_{n=1}^{N_s}\left|\frac{T(s_n)}{T_{\max}}\right|^2\right]^{\frac{1}{2}}, \tag{3.2}$$

where $T(s_n)$ are the integrals (2.6) evaluated at $s = s_n = n/N_s + 1$ (note that $T(0) = T(1) = 0$ always), while $T_{\max} = \max_{s,z}|\tau(s,z)|$. The integer N_s is chosen greater than N_T to eliminate problems of over-determination, and we typically used $N_s = 20$ for $N_T = 7$; the results are very little affected by other choices; greater accuracy is achieved for larger N_T as might be expected. Clearly T_S must be made as small as possible to allow (2.6) to be satisfied as nearly as possible.

In order to evaluate the integrals in (3.2), we must interpolate A and B onto a cylindrical mesh. This is achieved by first finding a least-squares fit to

$$\left.\begin{aligned} &\sum_{m=1}^{N_\theta}\sum_{n=1}^{N_r-1} b_{mn} j_{2m}(\alpha_{mn} r) P_{2m}^1(\cos\theta) \quad \text{for } B, \\ \text{and} \quad &\sum_{m=0}^{N_\theta-1}\sum_{n=1}^{N_r} a_{mn} j_{2m+1}(\alpha_{mn} r) P_{2m+1}^1(\cos\theta) \quad \text{for } A, \end{aligned}\right\} \tag{3.3}$$

where the j_k are spherical Bessel functions and the α_{mn} are the first N_r solutions of the equation

$$j_{2m}(x) = 0. \tag{3.4}$$

The choice of coefficients in (3.3) clearly shows that the poloidal field is of dipole type, and it may easily be shown that such representations automatically satisfy the boundary conditions on A and B at $r = 1$. It was usually found to be sufficient to choose N_θ and N_r both equal to 6 when the number of mesh points used to represent A and B in the upper hemisphere was 64. The series (3.3) have the advantage that they can be differentiated explicitly and evaluated at any point, so that the integrands for (3.2) can be found. Thus T_S can be evaluated for any values of the coefficients G_n and then, using a standard package, minimized with respect to variations in the G_n. As expected, the initial guess for U_G made no difference to the final solution. This procedure determines the G_n uniquely, and U_G can then be found by integrating (3.1) with respect to s and setting $U_G(1) = 0$ for definiteness. The

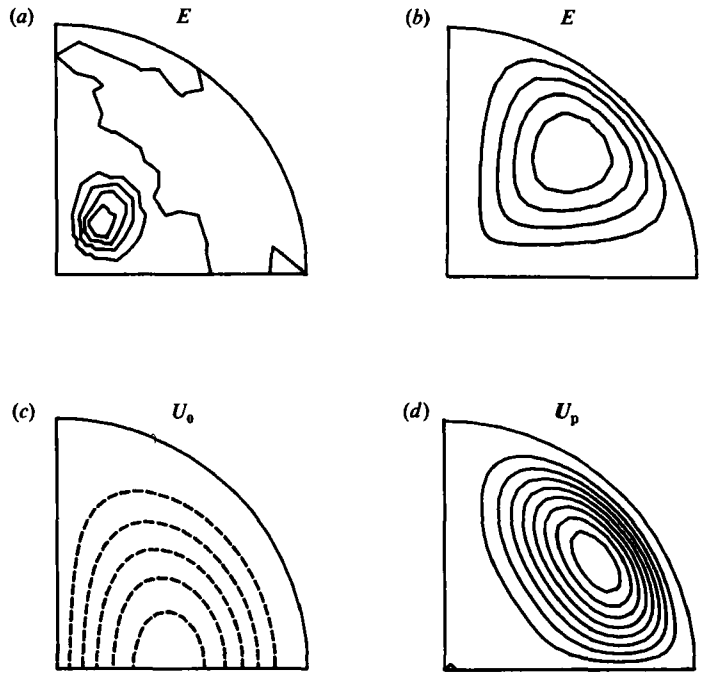

FIGURE 1. the e.m.f. from non-axisymmetric convection (see Fearn & Proctor 1984), a chosen e.m.f. $E = 16r^2(1-r^2)\sin^2\theta\cos^2\theta$ and the toroidal flow $U_0 = -(25\sqrt{5}/16)\, r(1-r^2)^2\sin\theta$ used in our calculations are illustrated in (*a*)–(*c*) respectively by contour plots of their strengths in the quadrant $0 \leqslant r \leqslant 1, 0 \leqslant \theta \leqslant \frac{1}{2}\pi$. Broken contour lines correspond to negative values of the function. Streamlines of the poloidal flow $\boldsymbol{U}_p = \boldsymbol{\nabla}\times\boldsymbol{\nabla}\times S\boldsymbol{r}$ with $S = 2.5\, R_m^p r^6(1-r)^2\,(3\cos 2\theta + 1)$ are shown in (*d*). The flow direction indicated is that corresponding to positive values of R_m^p.

procedure seems to work well apart from some difficulties near $s = 1$ due to the fact that $T(s) \to 0$ [since the height of the cylinder $C(s)$ tends to zero], as $s \to 1$ whatever the zonal flow. These problems are resolved and discussed in the next section and we show that our method yields converged solutions that satisfy (2.6) to acceptable accuracy.

4. Results and discussion

4.1 *Some typical solutions*

All the solutions reported in this paper are based on the prescribed flow fields shown in figure 1. Both the zonal velocity and poloidal flow field (whose dimensionless amplitude is arbitrary and measured by the parameter R_m^p) are given simple forms so as to maximize the resolution of the fields obtained with a given number of mesh points. Other velocity fields have been investigated, but solutions seem to be available in every case. The fields of figure 1 are the same as those used in FP84 and FP87. We also use one or other of the two e.m.f. profiles shown in figure 1. Profile (*a*) is taken directly from a converged calculation for the full convective problem (but without satisfying Taylor's constraint) described in FP87. Note that it is confined to a small region inside the sphere, as a result of the field concentration at larger R_m described by Fearn & Proctor (1983*a*, *b*). To provide contrast, and also for better resolution, profile (*b*) fills the sphere. The amplitudes of the e.m.f. and zonal flow profiles are arbitrary, since varying them serves only to change the absolute and

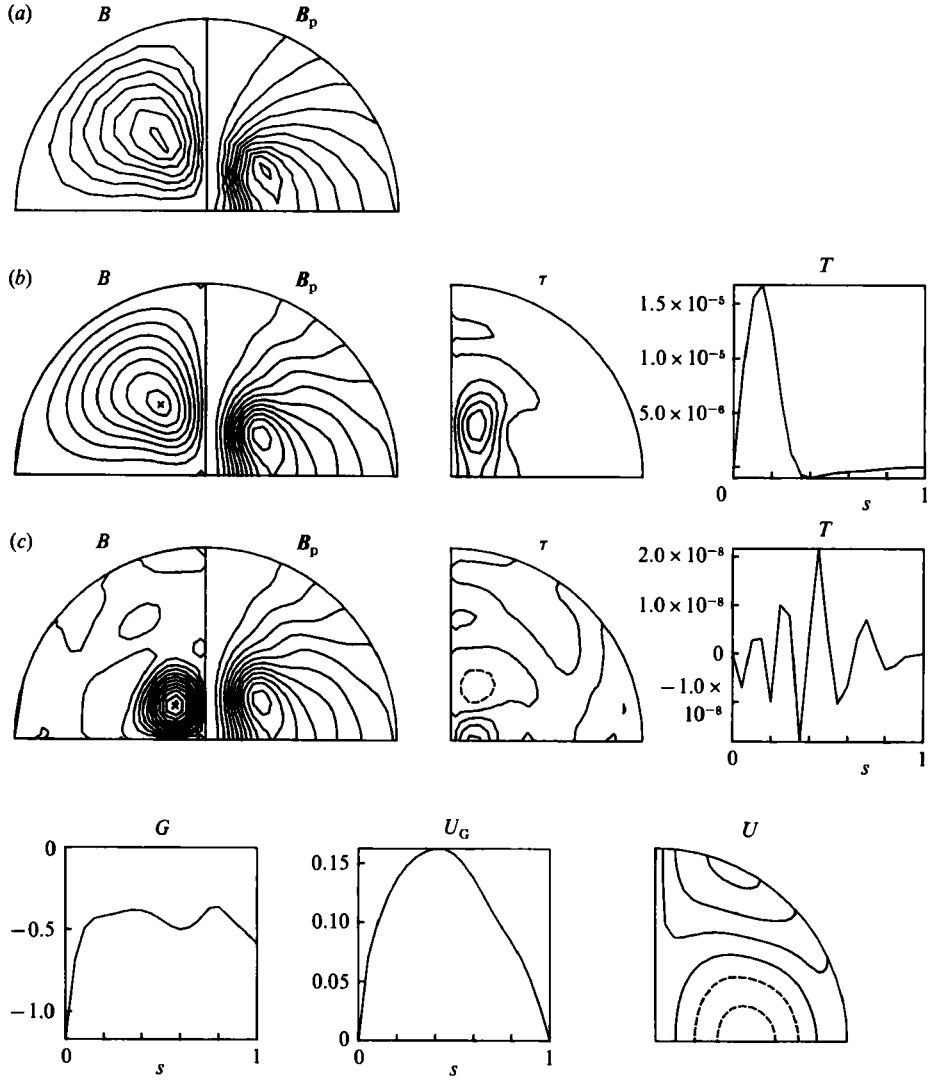

FIGURE 2. In (*a*) is shown the dipole field which is generated by the e.m.f. E_ϕ illustrated in figure 1 (*a*) and the toroidal flow U_0 illustrated in figure 1 (*c*). There is no poloidal flow. Poloidal field lines and contours of the toroidal field strength are shown. The finite-difference calculations used step lengths of $h_r = 1/N$ in r and $h_\theta = \pi/2L$ in θ, with $N = L = 8$. The field is then fitted to the series (3.3) with $N_r = N_\theta = 6$. The fitted field is plotted in (*b*) using a 20×20 (s, z) grid together with the corresponding azimuthal component of the Lorentz force $\tau(s, z)$ and its integral over z, $T(s)$, see (2.6). The contour interval for $\tau(s, z)$ in both (*b*) and (*c*). Clearly in (*b*), the Taylor constraint $T(s) = 0$ is not satisfied: $T_S = 2$. In (*c*) we show how the solution shown in (*b*) is modified when the geostrophic flow is chosen to satisfy the Taylor constraint. The toroidal flow appears only in the equation determining the toroidal field, so the poloidal field is unchanged. The toroidal field is now concentrated in the region where the poloidal field is approximately aligned with the rotation axis. Regions of positive τ cancel regions of negative τ to give a T_S which is three orders of magnitude smaller than that in (*b*); $T_S = 7 \times 10^{-3}$. Also shown is the geostrophic flow (both $G = s\Omega_G'$ and U_G are illustrated) together with the total toroidal flow $U = U_0 + U_G$. The latter may be compared with U_0 which is illustrated in figure 1 (*c*). The geostrophic flow is represented by the sum (3.1) with seven terms in the Chebyshev series for $0 \leqslant s \leqslant s_0$. For $s_0 < s \leqslant 1$, we take G' to be a constant; its value at $s = s_0$. Here $s_0 = 0.8$. The arbitrary uniform rotation is chosen to make $U_G = 0$ at $s = 1$. The value of s_0 is chosen to eliminate the 'tail' which may appear near $s = 1$, see figure 4.

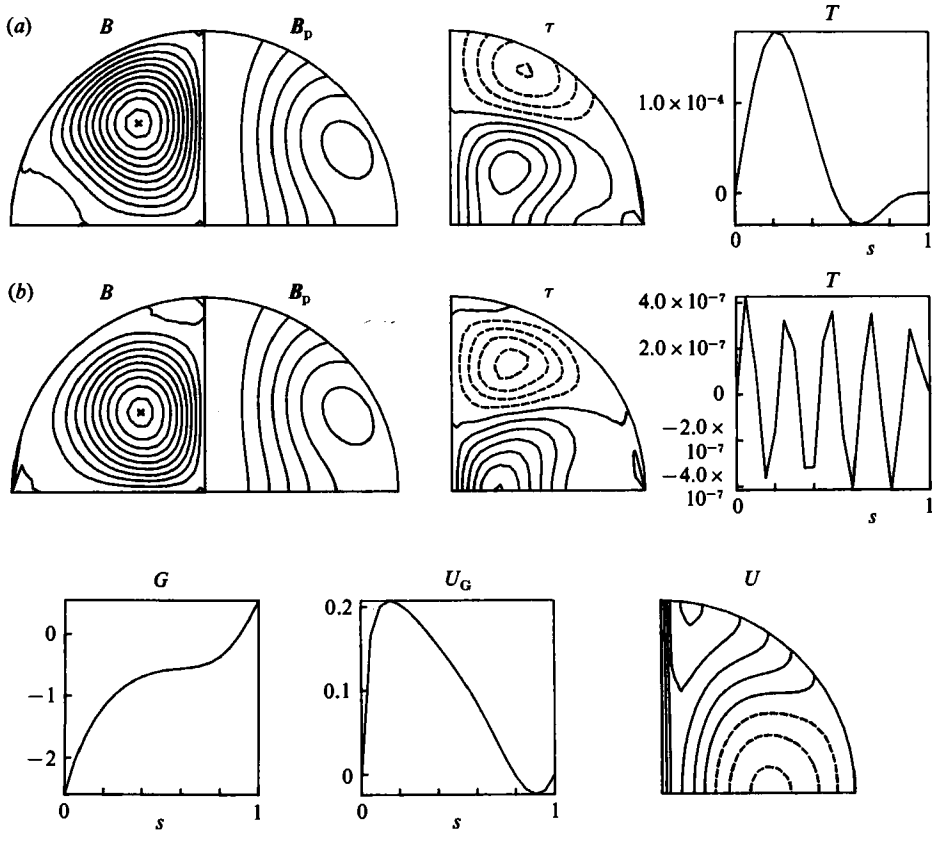

FIGURE 3. As figure 2(*b*, *c*) but for the e.m.f. in figure 1(*b*), $N = L = 15$, $N_r = N_\theta = 8$, and $s_0 = 1$. In (*a*), $T = 0.3$; in (*b*) $T_S = 10^{-3}$. The contour interval for τ is 2×10^{-4} for both (*a*) and (*b*).

relative magnitudes of A and B (and in the latter case, the magnitude of Ω_G) without changing their functional forms.

In figure 2(*a*) we show the 'raw' field that emerges as the solution of (2.5) with the e.m.f. profile (*a*) and zero poloidal flow. This can be compared with the 'fitted' field as defined in (3.3) and shown in figure 2(*b*) which can be seen to provide a good representation. Also shown are a contour plot of $\tau(s, z)$ and a graph showing $T(s_n)$, $n = 1 \ldots N_s$. Clearly for most s_n, $T(s_n)$ is of the order of the size of the integrand so that Taylor's condition is not even approximately satisfied. In contrast figure 2(*c*) shows the effect of choosing Ω_G to minimize T_S. It can be seen that the values of $T(s_n)$ are now of the order of 10^{-3} times the maximum value of the integrand, so that $T_S = 10^{-3}$. Also shown are $G(s)$ and $U_G(s) \equiv s\Omega_G(s) = -s\int_s^1 (1/s')\, G(s')\, ds'$; and contours of the total toroidal velocity $U = U_0 + U_G$. Replacing the e.m.f. profile (*a*) with (*b*) gives the solutions illustrated in figures 3(*a*, *b*). Comparing the two cases we see that the size of U_G is comparable with that of U in both cases, but the manner in which T_S is made small seems very different. For profile (*a*) the effect of Ω_G is to make B significant only near the centre of the sphere, where B_{ps} is rather small. [It can be seen that this is advantageous from the alternative representation (2.11) of (2.6).] In contrast, for profile (*b*) the change in the toroidal field is relatively very small and yet the change in the $T(s_n)$ is very significant. Here, it seems the minimization can be achieved by matching regions of positive B_{ps} with ones of negative B_{ps} that

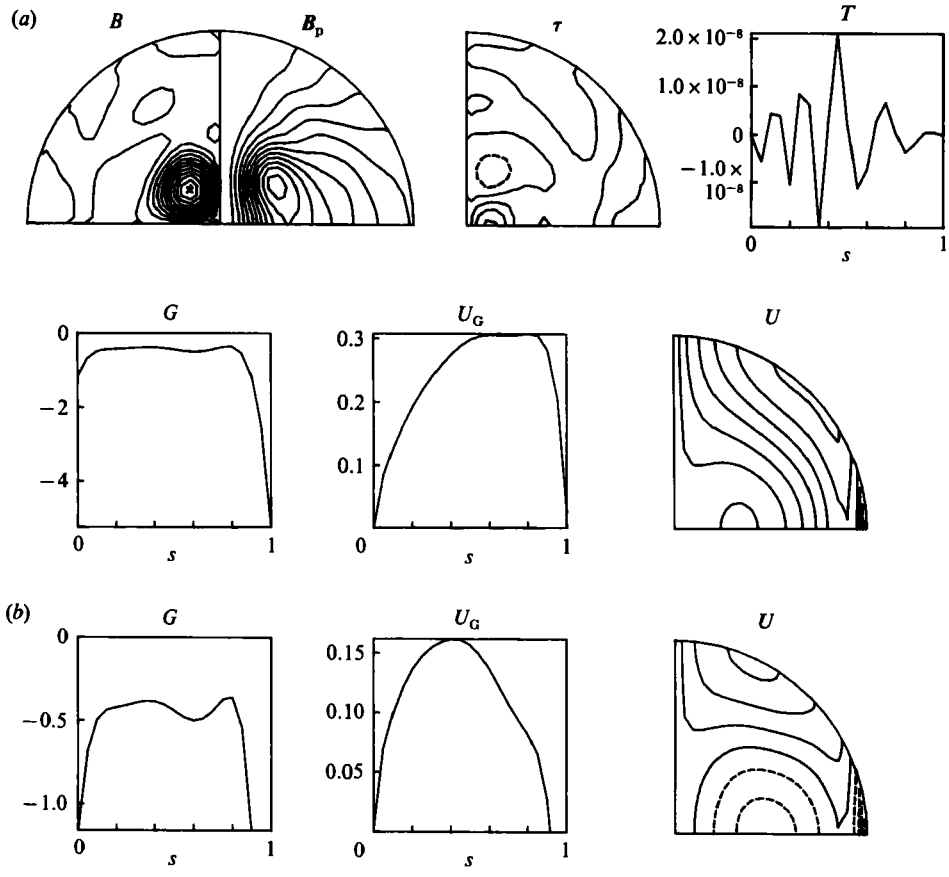

FIGURE 4. In (*a*) is shown a repeat of the calculation of figure 2(*c*), but with $s_0 = 1$. The solution for B, and hence for τ, is virtually indistinguishable from that shown in figure 2(*c*), but the solution for U_G looks quite different. This apparent difference is due to the large change in U_G near $s = 1$, and the consequent rescaling of the graphs. In (*b*) we redraw the toroidal flows shown in (*a*) on the same scales as the corresponding flows in figure 2(*c*). The arbitrary uniform rotation is chosen so that U_G has the same maximum value in both cases. It can now be seen that the geostrophic flow here is identical with the geostrophic flow in figure 2(*c*) for $0 \leqslant s \leqslant 0.8$. The geostrophic flow is quite different for the two cases for $0.8 < s \leqslant 1$. Since the solution for B is unaltered, this demonstrates that U_G in the region close to $s = 1$ is poorly determined by our minimization procedure of satisfying the Taylor constraint.

have similar values of B. [Note that even with no geostrophic flow there is considerable cancellation between regions of positive and negative $\tau(s, z)$ for profile (*b*).] The structure of the induced geostrophic flow is unremarkable in both cases, though each shows the logarithmic singularity in the shear at $s = 0$ predicted in §2.

4.2. *The 'tail' of* Ω_G *at* $s = 1$

It has already been noted that $T(s)$ vanishes identically at $s = 0$ and $s = 1$. In the former case the reason is simply tat both A and B vanish on the axis of symmetry. In the latter it is because the height of the cylinder $C(s)$ tends to zero there. One might thus expect that details of the magnetic field near $s = 1$ would have little effect on T_S, implying that Ω_G is poorly determined there (at least inasmuch as Ω_G is determined locally). This effect was observed in the earlier runs we made, using the

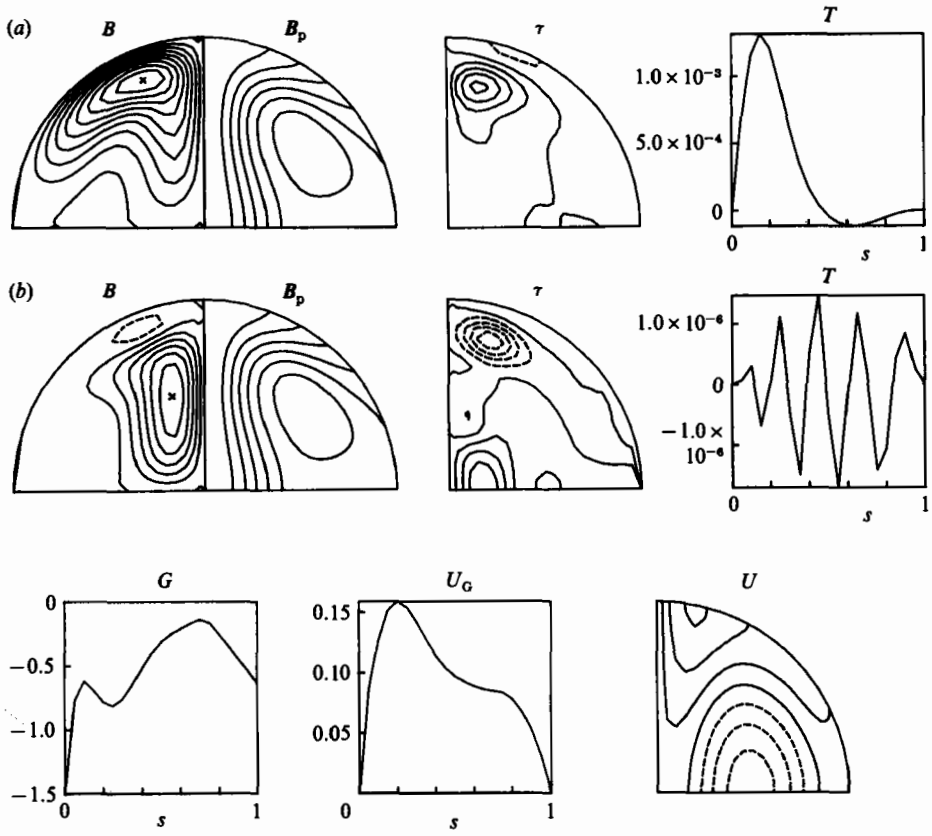

FIGURE 5. As figure 3, but with a poloidal flow U_p [as illustrated in figure 1*d*]; $R_m^p = 20$, and $s_0 = 0.75$. (*a*) $T_S = 1$; (*b*) $T_S = 4 \times 10^{-3}$.

representation (3.1) in $0 < s < 1$, where the minimizing form of $G(s)$ possessed an anomalous tail near $s = 1$. We attempted to conteract this by introducing a different weighting of the $T(s_n)$ in T_S so as to give more prominence to larger values of s, but this only resulted in a 'solution' which satisfied the constraints less well at smaller values. This is to be expected on physical grounds, since clearly the region of small s is the most important in determining the B-field. We therefore decided to use (3.1) only for $0 < s < s_0$ (where $s_0 = 0.8$ in the present case) and to achieve a smooth profile for $s_0 < s < 1$ by fitting a function of the form $G(s) = a + Bs$ in this region so that $G(s_0)$, $G'(s_0)$ are continuous. The effectiveness of this procedure can be judged for particular cases by comparing figure 2(*c*) ($s_0 = 0.8$) with figure 4 ($s_0 = 1$). It can be seen that the toroidal field and $G(s)$ agree closely for $s < s_0$, as one might expect, justifying the second procedure, which is thus used throughout the paper. The choice of s_0 is determined by the size of the tail, but its precise value is not crucial.

4.3. *The role of the poloidal flow*

Figures 5 and 6 show, for the e.m.f. profile (*b*), two solutions for the poloidal flow in figure 1(*d*), with $R_m^p = 20$ and -20, respectively. These should be compared with the corresponding solution for profile (*b*) in figure 3, where $R_m^p = 0$. The poloidal velocity field is normalized so that the maximum (dimensionless) speed is R_m^p. We would not expect R_m^p to be very large if our ideas on the scaling of the poloidal relative

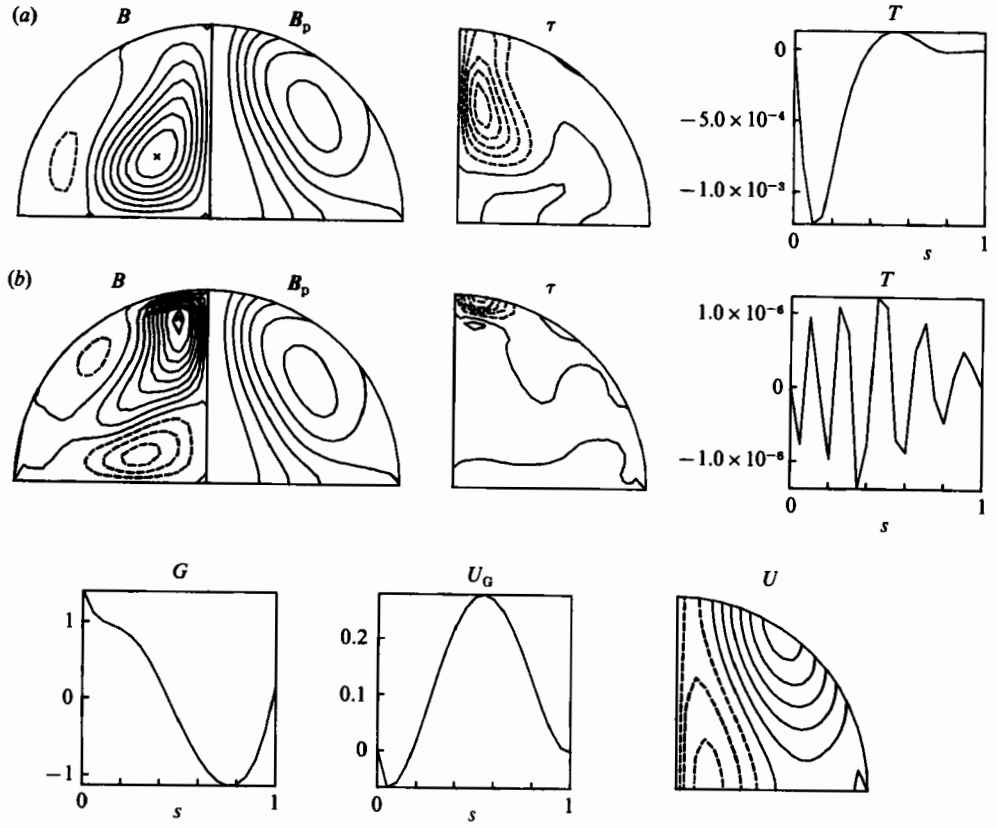

FIGURE 6. As figure 5, but with $R_m^p = -20$, and $s_0 = 1$. (a) $T_S = 1$; (b) $T_S = 3\times10^{-3}$.

to the toroidal field (as given in §2) are correct. On the other hand, if $|R_m^p|$ is too small no significant effect on Ω_G is observed.

In the case $R_m^p = +20$, the effect of U_p is to increase B_p near the axis and decrease it near $s = 1$. One might then expect the toroidal field to arrange itself to be larger for points away from the axis, but B is itself subject to the same advection effect as A. The net result is a strong, but essentially one-signed field close to the axis. T_S is about 4 times as large for $R_m^p = 20$ as for $R_m^p = 0$ with the same truncations, pointing to a more complicated structure for U_G, though this is chiefly manifested in the graph of $G(s)$. The case $R_m^p = -20$ is completely different, with both B_p and B being advected into the region near the pole. A significant region of reversed field appears at the equator and U_G looks completely different. The plot of $\tau(s, z)$ in this case suggests there may be some resolution difficulty near the poles, but we do not anticipate that a more accurate calculation will change the solutions for U_G noticeably.

5. Conclusion

We have shown in previous sections that, for a given mean e.m.f. and poloidal mean velocity (which is to say for a given axisymmetric poloidal magnetic field) and a given non-geostrophic zonal flow field, an additional geostrophic flow may be determined uniquely such that the resulting toroidal magnetic field satisfies Taylor's constraint

(2.6). By fixing the e.m.f., rather than writing $E = \alpha B$ and fixing α, we have transformed the problem from a transcendentally nonlinear one (essentially an eigenvalue problem for the magnitude of α, subject to an infinite number of constraints that determine U_G – see the discussion in Malkus & Proctor 1975) to one that is linear and thus much more tractable. While it is known that the problem posed in terms of α may not always have solutions, here we have found no cases where solutions are impossible, or non-smooth. The manner in which Taylor's condition is satisfied (in general by producing a B that is relatively large where B_{ps} is small) raises some intriguing parallels with the work of Braginskii (1975, 1978), whose 'model Z' description of the geodynamo relies on B_{ps} being small throughout the region where B is significant. The motivation for our model is of course quite different since (in contrast to Braginskii) we see only a passive, rather than a dominating role for the Ekman layer that will arise at $r = 1$ to accommodate the no-slip condition there.

In FP87 we describe our attempts to incorporate the scheme described in the present paper into a self-consistent dynamo iteration. Though no converged solutions have yet emerged, the stage of the iteration presented here was always accomplished successfully. The next stage is to take into account the mean Lorentz forces due to fluctuating fields. This remains a much more demanding task, and while Soward (1986) has made some progress recently in a plane layer model, there are to date no self-consistent solutions in a spherical geometry, nor have any mean magnetic fields been investigated that arise (as in FP87) from the dynamo process itself. Such an extension remains a challenging topic for future work.

This research was supported by the Science and Engineering Research Council of Great Britain.

REFERENCES

Braginskii, S. I. 1964*a* Kinematic models of the Earth's hydromagnetic dynamo. *Geomag. Aeron.* **4**, 572–683.

Braginskii, S. I. 1964*b* Magnetohydrodynamics of the Earth's core. *Geomag. Aeron.* **4**, 698–711.

Braginskii, S. I. 1975 Nearly axially symmetric model of the hydromagnetic dynamo of the Earth I. *Geomag. Aeron.* **15**, 122–128.

Braginskii, S. I. 1978 Nearly axially symmetric model of the hydromagnetic dynamo of the Earth II. *Geomag. Aeron.* **18**, 225–231.

Childress, S. 1969 A class of solutions of the magnetohydrodynamic dynamo problem. In *Applications of Modern Physics to the Earth and Planetary Interiors* (ed. S. K. Runcorn), p. 629. Wiley-Interscience.

Fearn, D. R. & Proctor, M. R. E. 1983*a* Hydromagnetic waves in a differentially rotating sphere. *J. Fluid Mech.* **128**, 1–20.

Fearn, D. R. & Proctor, M. R. E. 1983*b* The stabilizing role of differential rotation on hydromagnetic waves, *J. Fluid Mech.* **128**, 21–36.

Fearn, D. R. & Proctor, M. R. E. 1984 Self-consistent dynamo models driven by hydromagnetic instabilities, *Phys. Earth Planet Int.* **36**, 78–84.

Fearn, D. R. & Proctor, M. R. E. 1987 Self-consistent hydromagnetic dynamos. *Geophys. Astrophys. Fluid Dyn.* (to appear).

Greenspan, H. P. 1974 On α-dynamos. *Stud. Appl. Maths* **43**, 35–39.

Ierley, G. 1985 Macrodynamics of α^3-dynamos. *Geophys. Astrophys. Fluid Dyn.* **34**, 143–173.

Malkus, W. V. R. & Proctor, M. R. E. 1975 The macrodynamics of α-effect dynamos in rotating fluid systems. *J. Fluid Mech.* **67**, 417–444.

Moffatt, H. K. 1978 *Magnetic Field Generation in Electrically Conducting Fluids.* Cambridge University Press.

PROCTOR, M. R. E. 1975 Nonlinear mean field dynamo models and related topics. PhD thesis, University of Cambridge.

PROCTOR, M. R. E. 1977 Numerical solutions of the nonlinear α-effect dynamo equations, *J. Fluid Mech.* **80**, 769–784.

SOWARD, A. M. 1986 Nonlinear marginal convection in a rotating magnetic system. *Geophys. Astrophys. Fluid Dyn.* **35**, 329–371.

SOWARD, A. M. & JONES, C. A. 1983 α^2-dynamos and Taylor's constraint, *Geophys. Astrophys. Fluid Dyn.* **27**, 87–122.

TAYLOR, J. B. 1963 The magnetohydrodynamics of a rotating fluid and the earth's dynamo problem. *Proc. R. Soc. Lond.* A **274**, 274–283.